JACC: CARDIOVASCULAR IMAGING VOL. 16, NO. 4, 2023

ORIGINAL RESEARCH

Multi-Imaging Characterization of Cardiac Phenotype in Different Types of Amyloidosis

Adam Ioannou, MBBS, BSc,[a,*] Rishi K. Patel, MBBS, BSc,[a,*] Yousuf Razvi, MBChB,[a] Aldostefano Porcari, MD,[a] Daniel Knight, PhD,[a] Ana Martinez-Naharro, PhD,[a] Tushar Kotecha, PhD,[a] Lucia Venneri, MD, PhD,[a] Liza Chacko, MBBS, BSc,[a] James Brown, MB BChir,[a] Charlotte Manisty, MD, PhD,[b] James Moon, MD, PhD,[b] Brendan Wisniowski,[a] Helen Lachmann, MD,[a] Ashutosh Wechelakar, MD,[a] Carol Whelan, MD,[a] Peter Kellman, PhD,[c] Philip N. Hawkins, MD, PhD,[a] Julian D. Gillmore, MD, PhD,[a,†] Marianna Fontana, MD, PhD[a,†]

ABSTRACT

BACKGROUND Bone scintigraphy is extremely valuable when assessing patients with suspected cardiac amyloidosis (CA), but the clinical significance and associated phenotype of different degrees of cardiac uptake across different types is yet to be defined.

OBJECTIVES This study sought to define the phenotypes of patients with varying degrees of cardiac uptake on bone scintigraphy, across multiple types of systemic amyloidosis, using extensive characterization comprising biomarkers as well as echocardiographic and cardiac magnetic resonance (CMR) imaging.

METHODS A total of 296 patients (117 with immunoglobulin light-chain amyloidosis [AL], 165 with transthyretin amyloidosis [ATTR], 7 with apolipoprotein AI amyloidosis [AApoAI], and 7 with apolipoprotein AIV amyloidosis [AApoAIV]) underwent deep characterization of their cardiac phenotype.

RESULTS AL patients with grade 0 myocardial radiotracer uptake spanned the spectrum of CMR findings from no CA to characteristic CA, whereas AL patients with grades 1 to 3 always produced characteristic CMR features. In ATTR, the CA burden strongly correlated with myocardial tracer uptake, except in Ser77Tyr. AApoAI presented with grade 0 or 1 and disproportionate right-sided involvement. AApoAIV always presented with grade 0 and characteristic CA. AL grade 1 patients (n = 48; 100%) had characteristic CA, whereas only ATTR grade 1 patients with Ser77Tyr had characteristic CA on CMR (n = 5; 11.4%). After exclusion of Ser77Tyr, AApoAI, and AApoAIV, CMR showing characteristic CA or an extracellular volume of >0.40 in patients with grade 0 to 1 cardiac uptake had a sensitivity and specificity of 100% for AL.

CONCLUSIONS There is a wide variation in cardiac phenotype between different amyloidosis types across different degrees of cardiac uptake. The combination of CMR and bone scintigraphy can help to define the diagnostic differentials and the clinical phenotype in each individual patient. (J Am Coll Cardiol Img 2023;16:464–477) © 2023 The Authors. Published by Elsevier on behalf of the American College of Cardiology Foundation. This is an open access article under the CC BY-NC-ND license (http://creativecommons.org/licenses/by-nc-nd/4.0/).

From the [a]National Amyloidosis Centre, University College London, Royal Free Campus, London, United Kingdom; [b]St Bartholomew's Hospital, London, United Kingdom; and the [c]National Heart, Lung, and Blood Institute, National Institutes of Health, Bethesda, Maryland, USA. *Drs Ioannou and Patel are joint first authors. †Drs Gillmore and Fontana are joint senior authors.

The authors attest they are in compliance with human studies committees and animal welfare regulations of the authors' institutions and Food and Drug Administration guidelines, including patient consent where appropriate. For more information, visit the Author Center.

Manuscript received February 23, 2022; revised manuscript received July 1, 2022, accepted July 7, 2022.

ISSN 1936-878X https://doi.org/10.1016/j.jcmg.2022.07.008

Cardiac amyloidosis (CA) is an increasingly recognized cause of heart failure for which there are specific treatments.[1,2] Several amyloid fibril proteins or "amyloid types" deposit in the heart and cause CA, but the vast majority of the cases are represented by light-chain amyloidosis (AL) and transthyretin amyloidosis (ATTR), the latter now probably more frequently diagnosed than the former. Less common although increasingly recognized causes of CA apolipoprotein AI amyloidosis (AApoAI) and apolipoprotein AIV amyloidosis (AApoAIV).[3,4] Establishing the correct amyloid fibril type is a mandatory step to administer appropriate treatment, which is critically dependent on the type of amyloid.

The utility of bone scintigraphy in the noninvasive diagnosis of ATTR-CA[5] has been associated with a significant increase in the use of the technique in the diagnostic pathway of CA, being currently performed not only in patients with ATTR but across a wide range of amyloid types. Indeed, low-grade cardiac uptake has been demonstrated in up to 40% of AL patients,[6] and an increasing number of patients with ATTR have been reported with low-grade cardiac uptake.[7] At present, the data on ^{99m}technetium-labeled 3,3-diphosphono-1,2-propanodicarboxylic acid (^{99m}Tc-DPD) uptake or, indeed, cardiac phenotype in AApoAI and AApoAIV is sparse, with the majority of available literature being case reports and small case series.[8-10] However, although the significance of grade 2 and 3 cardiac uptake in the absence of a plasma cell dyscrasia has been well defined, the phenotypic characterization of patients with CA with different degrees of cardiac uptake on bone scintigraphy across the spectrum of systemic amyloidosis has not been well established, leaving a knowledge gap in the clinical significance and associated clinical phenotype of different degrees of cardiac uptake across the different types of CA.

The aim of this study was to define the phenotypes of patients with varying degrees of cardiac uptake on bone scintigraphy, across multiple types of systemic amyloidosis, using extensive characterization comprising biomarkers as well as echocardiography and cardiac magnetic resonance (CMR).

METHODS

PATIENT POPULATION. We performed a retrospective search of the National Amyloidosis Centre database to identify all patients with confirmed amyloidosis between 2010 and 2021 who underwent ^{99m}Tc-DPD scintigraphy and CMR with intravenous gadolinium contrast at our center. Only newly diagnosed patients who were treatment naive were included in the study. The aim of this study was to define the phenotypes of patients with varying degrees of ^{99m}Tc-DPD cardiac uptake, across multiple types of systemic amyloidosis. For each degree of cardiac uptake, all cases from the National Amyloidosis Centre database were included if there were 50 or fewer cases, and a random sample was selected if there were more than 50 cases, as follows: 1) systemic AL (grade 0 cardiac uptake: n = 50; grade 1 cardiac uptake: n = 48; grade 2 cardiac uptake: n = 10; grade 3 cardiac uptake: n = 9); 2) ATTR (grade 0 cardiac uptake: n = 21; grade 1 cardiac uptake: n = 44; grade 2 cardiac uptake: n = 50; grade 3 cardiac uptake: n = 50); 3) AApoAI (grade 0 cardiac uptake: n = 3; grade 1 cardiac uptake: n = 4); and 4) AApoAIV (grade 0 cardiac uptake: n = 7). The patient selection process is outlined in **Figure 1** and the Supplemental Methods.

Diagnoses were confirmed based on validated diagnostic criteria.[11,12] In brief, all biopsy specimens were stained with Congo red dye and viewed under cross-polarized light. The definitive amyloid fibril type was established by immunohistochemical staining of amyloid deposits using monospecific antibodies and/or by microdissection of amyloid deposits and proteomic analysis, as previously described.[5] The diagnosis of AL was confirmed by central review of histology.

The diagnosis of ATTR-CA in patients with grade 1 ^{99m}Tc-DPD cardiac uptake was based on either: 1) endomyocardial biopsy proof of ATTR-amyloid deposits (5/44); 2) a pathogenic *TTR* sequence variant and no evidence of a plasma cell dyscrasia (17/44, 12 of which had extracardiac biopsy proof of ATTR) and no visceral organ uptake on serum amyloid P component (SAP) scintigraphy; or 3) extracardiac biopsy result positive for ATTR-amyloid and no visceral uptake on SAP scintigraphy (22/44). In patients with grade 2 or 3 ^{99m}Tc-DPD cardiac uptake, a diagnosis was based on either: 1) endomyocardial biopsy proof of ATTR-amyloid (17/100); 2) ATTR-amyloid in an extracardiac biopsy and no visceral uptake on SAP

ABBREVIATIONS AND ACRONYMS

AApoAI = apolipoprotein AI amyloidosis

AApoAIV = apolipoprotein AIV amyloidosis

AL = immunoglobulin light-chain amyloidosis

ATTR = transthyretin amyloidosis

CA = cardiac amyloidosis

CMR = cardiac magnetic resonance

ECV = extracellular volume

LGE = late gadolinium enhancement

LS = longitudinal strain

LV = left ventricle

LVEF = left ventricular ejection fraction

MWT = maximal wall thickness

RA = right atrium

RV = right ventricle

SAP = serum amyloid P component

SPECT = single-photon emission computed tomography

^{99m}Tc-DPD = ^{99m}technetium-labeled 3,3-diphosphono-1,2-propanodicarboxylic acid

JACC: CARDIOVASCULAR IMAGING, VOL. 16, NO. 4, 2023
APRIL 2023:464–477

FIGURE 1 Flowchart Demonstrating the Selection of Patients for the Study

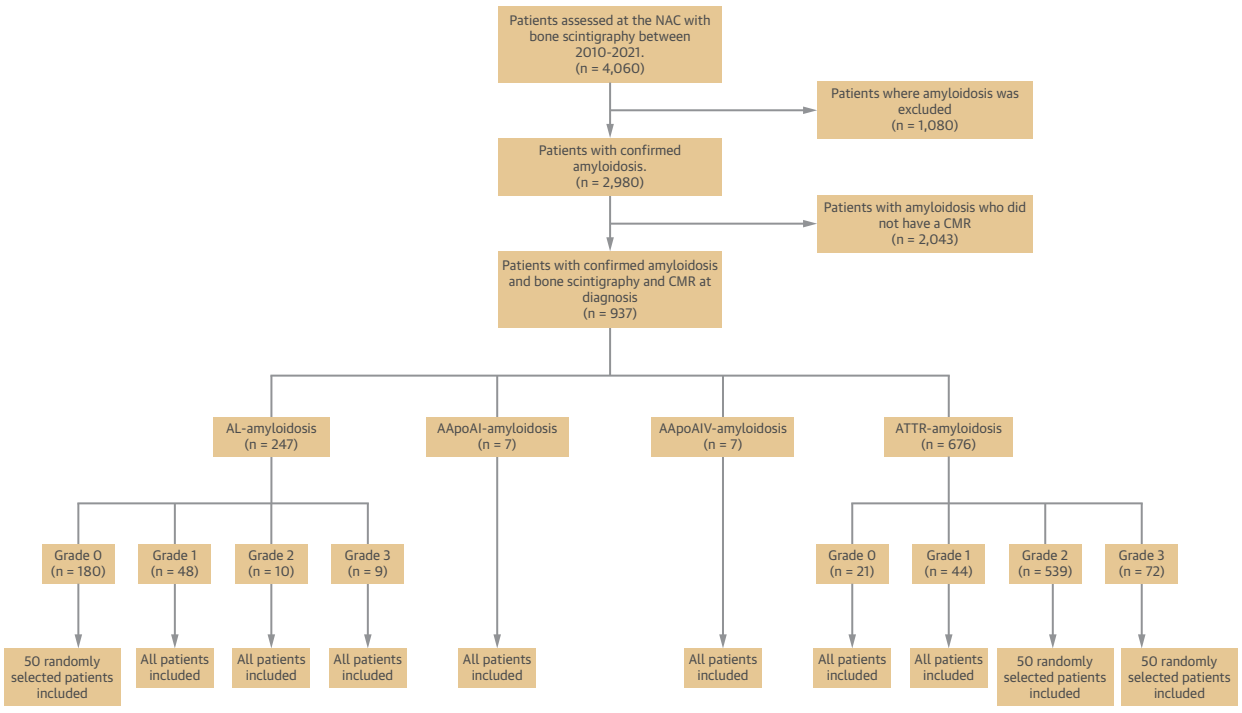

The flowchart shows how patients were selected for inclusion in the study. AApoAI = apolipoprotein AI amyloidosis; AApoAIV = apolipoprotein AIV amyloidosis; AL = immunoglobulin light-chain amyloidosis; ATTR = transthyretin amyloidosis; CMR = cardiac magnetic resonance; NAC = National Amyloidosis Centre.

scintigraphy (12/100); or 3) the absence of an abnormal serum free light-chain ratio and monoclonal immunoglobulin in the serum and urine by immunofixation (71/100). All patients underwent sequencing of the *TTR* gene.[12] AApoAI was confirmed by identification of a pathogenic ApoAI gene sequence variant (7/7), with histologic evidence of AApoAI amyloid tissue infiltration in 5 cases. AApoAIV was confirmed by histologic evidence of AApoAIV amyloid tissue infiltration on either cardiac (4/7) or extracardiac biopsy (3/7). All CMR scans were scored using the following grading system: no features of CA (normal left ventricle [LV] mass, no late gadolinium enhancement [LGE], and normal extracellular volume [ECV]), early cardiac amyloid infiltration (normal LV mass, raised ECV, and/or subendocardial LGE), and characteristic of CA (increased LV mass, diffuse subendocardial or transmural LGE, altered gadolinium kinetics, and raised ECV).

A total of 20 healthy volunteers with no symptoms or past history of cardiovascular disease or cardiovascular risk factors underwent CMR imaging to establish normal measurement ranges.

Patients were treated in accordance with the Declaration of Helsinki and provided written informed consent for analysis and publication of their data (research ethics committee reference 21/PR/0620). A separate ethical approval was obtained for the recruitment of healthy volunteers (research ethics committee reference 17/SC/0077).

^{99m}Tc-DPD BONE SCINTIGRAPHY PROTOCOL AND IMAGE ANALYSIS. Images were acquired by using the Discovery model NM/CT 670 hybrid gamma camera (GE Healthcare). Patients were intravenously injected with approximately 700 MBq (18.9 mCi) of ^{99m}Tc-DPD. The protocol consisted of a planar whole-body acquisition performed at 3 hours after the injection, followed by single-photon emission computed tomography (SPECT) imaging of the thorax. A low-dose, noncontrast computed tomography scan was performed for attenuation correction and anatomic localization, generating a volume of interest for the whole heart. The intensity of myocardial uptake on the planar ^{99m}Tc-DPD scan was categorized as 0 to 3 according to the grading system described by Perugini et al.[13]

TABLE 1 Baseline Characteristics and Echocardiographic and CMR Parameters for Patients With AL and Grade 0 Cardiac Uptake by ^{99m}Tc-DPD Scintigraphy, Separated by CMR Characteristics

	No Cardiac Amyloidosis (n = 9)	Early Cardiac Infiltration (n = 10)	Characteristic Cardiac Amyloidosis (n = 31)	*P* Value
Baseline characteristics				
Age, y	72.68 ± 8.86	70.19 ± 8.98	72.02 ± 8.95	0.807
Male	6 (66.7)	9 (90.0)	23 (74.20)	0.458
NYHA functional class				
I	7 (77.8)[a,b]	2 (20.0)	2 (6.5)	<0.001
II	2 (22.2)[b]	7 (77.8)	24 (77.4)	
III	0 (0.0)	1 (10.0)	5 (16.1)	
IV	0 (0.0)	0 (0.0)	0 (0.0)	
NT-proBNP, pg/L	144 (85-396)[b]	2,463 (404-5,382)	5,564 (2,956-9,645)	<0.001
Troponin, ng/L	17 (9-26)[b]	46 (19-72)	75 (38-125)	<0.001
eGFR, mL/min/1.73 m^2	60 (60-87)	75 (54-90)	71 (57-90)	0.957
Diagnosis				
Endomyocardial biopsy	0 (0.0)	1 (10.0)	1 (3.2)	0.506
Extracardiac solid organ biopsy	5 (55.6)[b]	3 (30.0)	2 (6.5)	0.004
Bone marrow biopsy	4 (44.4)	4 (40.0)	15 (48.4)	0.893
Fat biopsy	0 (0.0)	2 (20.0)	13 (41.9)	0.040
Echocardiographic variables				
IVSd, mm	11.22 ± 1.20[b]	11.70 ± 2.06[c]	15.63 ± 2.08	<0.001
IVSd indexed, mm/m^2	5.74 ± 0.57[b]	6.24 ± 1.34[c]	8.45 ± 1.31	<0.001
PWTd, mm	11.11 ± 1.67[b]	11.30 ± 1.70[c]	15.57 ± 1.78	<0.001
PWTd indexed, mm/m^2	5.68 ± 0.59[b]	6.04 ± 1.28[c]	8.44 ± 1.29	<0.001
LS, %	−19.54 ± 3.04[b]	−17.63 ± 1.17[c]	−10.35 ± 3.27	<0.001
E/A	1.16 ± 0.94[b]	1.02 ± 0.61[c]	1.99 ± 0.98	0.002
E/e′ average	8.30 ± 2.95[b]	15.11 ± 5.29[c]	23.22 ± 8.30	<0.001
LAA indexed, cm^2/m^2	8.57 ± 1.35[b]	10.38 ± 2.92[c]	12.995 ± 2.42	<0.001
RAA indexed, cm^2/m^2	7.82 ± 1.45[b]	9.93 ± 2.49[c]	11.60 ± 2.91	0.004
CMR variables				
MWT, mm	10.11 ± 1.27[b]	11.90 ± 1.60[c]	17.40 ± 2.96	<0.001
MWT indexed, mm/m^2	5.19 ± 0.73[b]	6.35 ± 1.24[c]	9.49 ± 1.88	<0.001
LV mass indexed, g/m^2	63.40 ± 11.78[a,b]	85.80 ± 10.64[c]	114.19 ± 20.1	<0.001
SV indexed, mL/m^2	42.22 ± 7.74	38.80 ± 13.00	36.74 ± 8.29	0.298
EF, %	69.44 ± 5.68[b]	62.56 ± 7.61	55.58 ± 10.40	<0.001
MAPSE, mm	11.14 ± 2.19[b]	9.60 ± 1.43[c]	6.53 ± 2.10	<0.001
TAPSE, mm	21.56 ± 7.30[b]	17.11 ± 4.86[c]	11.50 ± 5.10	<0.001
LAA indexed, cm^2/m^2	12.22 ± 3.04[b]	12.16 ± 3.34[c]	16.53 ± 2.78	<0.001
RAA indexed, cm^2/m^2	12.21 ± 3.26	11.31 ± 2.44	13.43 ± 2.53	0.078
Native myocardial T1	1,005 ± 41[a,b]	1,077 ± 46[c]	1,182.32 ± 59.35	<0.001
Myocardial T2	47.44 ± 3.71[a,b]	50.80 ± 3.16	52.19 ± 3.02	<0.001
LV LGE				
None	10 (100.0)[a,b]	0 (0.0)	0 (0.0)	<0.001
Subendocardial	0 (0.0)[a]	10 (100.0)[c]	7 (43.8)	
Transmural	0 (0.0)[b]	0 (0.0)[c]	24 (77.4)	
RV LGE	0 (0.0)[a,b]	5 (50.0)	24 (77.4)	<0.001
ECV	0.28 ± 0.02[a,b]	0.38 ± 0.03[c]	0.55 ± 0.07	<0.001

Values are mean ± SD, n (%), or or median (IQR). *P* values for pairwise comparison: [a]$P < 0.05$ for no CA vs early CA. [b]$P < 0.05$ for no CA vs characteristic CA. [c]$P < 0.05$ for early CA vs characteristic CA.

AL = immunoglobulin light-chain amyloidosis; CA = cardiac amyloidosis; CMR = cardiac magnetic resonance; ECV = extracellular volume; EF = ejection fraction (calculated using the subtraction of LV volumes in CMR); eGFR = estimated glomerular filtration rate; IVSd = interventricular septum in diastole; LAA = left atrial area (measured in the 4-chamber view); LGE = late gadolinium enhancement; LS = longitudinal strain; LV = left ventricle; MAPSE = mitral annular plane systolic excursion; MWT = maximal wall thickness; NT-proBNP = N-terminal pro–B-type natriuretic peptide; NYHA = New York Heart Association; PWTd = posterior wall thickness in diastole; RAA = right atrial area (measured in the 4-chamber view); RV = right ventricle; SV = stroke volume; TAPSE = tricuspid annular plane systolic excursion; ^{99m}Tc-DPD = ^{99m}technetium-labeled 3,3-diphosphono-1,2-propanodicarboxylic acid.

JACC: CARDIOVASCULAR IMAGING, VOL. 16, NO. 4, 2023
APRIL 2023:464–477

SAP SCINTIGRAPHY. SAP scintigraphy was used to assess for visceral organ amyloid infiltration. Anterior and posterior whole-body images were acquired following ^{123}I SAP administration using a General Electric Infinia Hawkeye or Discovery 670 Gamma Camera with extended low-energy general-purpose collimators. Visceral amyloid burden was scored by visual assessment.[14]

ECHOCARDIOGRAPHY. All echocardiograms were performed and reviewed by experienced operators blinded to the final diagnosis and analyzed according to guidelines as previously described.[15]

CARDIAC MAGNETIC RESONANCE. All subjects underwent CMR on a 1.5-T clinical scanner (Magnetom Aera, Siemens Healthcare). Within a conventional clinical scan (localizers and cine imaging with a steady-state free-precession sequence), LGE imaging was acquired with both magnitude inversion recovery and phase-sensitive inversion recovery sequence reconstructions with steady-state free-precession readouts. T1 measurement was performed with the use of the modified look-locker inversion recovery sequence. After a bolus of gadoterate meglumine (0.1 mmol/kg, gadolinium-DOTA [Dotarem, Guerbet]) and LGE imaging, T1 mapping was repeated 15 minutes postcontrast using the same slice locations with the modified look-locker inversion recovery sequence to produce automated inline ECV mapping reconstruction. T1 mapping protocols used 5s(3s)3s and 4s(1s)3s(1s)2s sampling precontrast and postcontrast, respectively.[16,17]

The normal ECV range was calculated from the population of healthy volunteers (ECV: 0.27 ± 0.02; normal range 0.23-0.30).

STATISTICAL ANALYSIS. Statistical analysis was performed using IBM SPSS Statistics, version 25. All continuous variables were tested for normal distribution (Shapiro-Wilk test) and are presented as mean ± SD or median (IQR). Following analysis of healthy volunteer CMR images, normal ranges were calculated as the mean ± 2 × SD. The independent Student's *t*-test or its nonparametric equivalent (Mann-Whitney *U* test) were used to compare the distribution of 2 groups. The 1-way analysis of variance or its nonparametric equivalent (Kruskal-Wallis test) were used to compare the distribution of multiple groups, with a significant result followed by a post hoc Bonferroni-corrected pairwise comparison to establish where differences lay. Levene's test was used to check the homogeneity of variance in the Student's *t*-test and analysis of variance. Categoric data are presented as absolute numbers and frequencies (%) and compared using the chi-square test or Fisher exact test as appropriate. Prevalence results within subgroups are presented as a percentage, followed by the 95% CI, calculated using the 1-sample binomial test. Receiver-operating characteristic curves were constructed to establish ECV cutoffs for diagnosing AL and ATTR. The optimal cutoff value was defined as the point with the highest sum of sensitivity and specificity and was calculated using the Youden and Liu methods.

Correlation between ^{99m}Tc-DPD cardiac uptake and parameters of cardiac structure and function were assessed using Pearson's *r* or Spearman's rho. Statistical significance was defined as $P < 0.05$.

RESULTS

A total of 296 patients with amyloidosis and 20 healthy volunteers were included. There was a similar proportion of men among patients with systemic amyloidosis compared to healthy volunteers (77.6% vs 80.0%; $P = 0.803$), but the healthy volunteers were younger (71.45 ± 11.42 years vs 45.60 ± 7.20 years; $P < 0.001$). Within the amyloidosis cohort, 117 had AL, 165 had ATTR, 7 had AApoAI, and 7 had AApoAIV. Of those with ATTR, 85 had wild-type transthyretin amyloidosis and 80 had hereditary transthyretin amyloidosis (V122I: n = 27; T60A: n = 22; V30M: n = 12; Ser77Tyr: n = 8; G6s: n = 2; D39V: n = 1; E54G: n = 1; E54L: n = 1; E89K: n = 1; F44L: n = 1; Glu89Lys: n = 1; Ile107phe: n = 1; L12P: n = 1; V201: n = 1).

IMMUNOGLOBULIN LIGHT-CHAIN AMYLOIDOSIS. All patients with AL (n = 117) had either elevated kappa or lambda free light chains and an abnormal kappa:lambda ratio, and 107 (91.5%; 95% CI: 84.8%-95.8%) had evidence of a paraprotein in the serum and/or urine (kappa: n = 25; lambda: n = 82). Extracardiac involvement assessed by SAP scintigraphy demonstrated that 62 (53.0%; 95% CI: 43.6%-62.3%) patients had evidence of only cardiac involvement, 20 (17.1%; 95% CI: 11.8%-25.2%) had liver involvement, 53 (45.3%; 95% CI: 36.1%-54.8%) had spleen involvement, and 18 (15.4%; 95% CI: 9.4%-23.2%) had renal involvement (of whom 7 had nephrotic syndrome).

In AL patients with grade 0 cardiac uptake, there were 9 (18.0%; 95% CI: 8.6%-31.4%) with no evidence of CA on CMR, 10 (20.0%; 95% CI: 10.0%-33.7%) with early cardiac amyloid infiltration, and 31 (62.0%; 95% CI: 47.2%-75.4%) with characteristic features of CA. AL patients with grade 0 cardiac uptake and no CMR features of CA had normal cardiac structure, function, and tissue characterization. AL patients with grade 0 cardiac uptake and

TABLE 2 Baseline Characteristics and Echocardiographic and CMR Parameters for Patients With AL and a Characteristic CMR Finding Across All ^{99m}Tc-DPD Scintigraphy Grades

	Grade 0 (n = 31)	Grade 1 (n = 48)	Grade 2 (n = 10)	Grade 3 (n = 9)	*P* Value
Baseline characteristics					
Age, y	72.02 ± 8.95	68.71 ± 10.29	73.38 ± 8.82	68.35 ± 8.47	0.303
Male	23 (74.2)	38 (79.2)	7 (70.0)	7 (78.7)	0.913
NYHA functional class					0.012
I	2 (6.5)	5 (10.4)	0 (0.0)	0 (0.0)	
II	24 (77.4)[a]	23 (47.9)	7 (70.0)	5 (55.6)	
III	5 (16.1)	19 (39.6)	1 (10.0)	4 (44.4)	
IV	0 (0.0)	1 (2.1)	2 (20.0)	0 (0.0)	
NT-proBNP, pg/L	5,564 (2,956-9,645)	5,664 (3,784-11,986)	5,882 (4,105-13,994)	7,662 (4,168-10,225)	0.875
Troponin, ng/L	75 (38-125)	100 (63-184)	123.0 (90.0-163.8)	96.5 (67.5-149.5)	0.112
eGFR, mL/min/1.73 m^2	71 (57-90)	66 (51-79)	53.5 (43.5-70.5)	62 (51.5-65.5)	0.126
Diagnosis					
Endomyocardial biopsy	1 (3.2)	7 (14.6)	3 (30.0)	1 (11.1)	0.137
Extracardiac solid organ biopsy	2 (6.5)	5 (10.4)	2 (20.0)	2 (22.2)	0.457
Bone marrow biopsy	15 (48.4)	16 (33.3)	4 (40.0)	1 (11.1)	0.200
Fat biopsy	13 (41.9)	20 (41.7)	1 (10.0)	5 (55.6)	0.190
Echocardiographic variables					
IVSd, mm	15.63 ± 2.08	15.75 ± 1.94	15.80 ± 2.90	17.00 ± 3.63	0.491
IVSd indexed, mm/m^2	8.45 ± 1.31	8.63 ± 1.28	8.41 ± 1.78	8.79 ± 2.53	0.907
PWTd, mm	15.57 ± 1.78	15.65 ± 2.01	15.50 ± 2.42	15.88 ± 2.48	0.980
PWTd indexed, mm/m^2	8.44 ± 1.29	8.55 ± 1.25	8.26 ± 1.65	8.18 ± 1.92	0.856
LS, %	−10.35 ± 3.27	−9.80 ± 2.77	−9.93 ± 2.38	−8.20 ± 3.63	0.350
E/A	1.99 ± 0.98	2.59 ± 1.34	2.74 ± 0.31	2.23 ± 1.23	0.273
E/e′ average	23.22 ± 8.30	20.26 ± 9.09	17.02 ± 4.31	21.75 ± 10.08	0.196
LAA indexed, cm^2/m^2	12.995 ± 2.42	12.81 ± 2.46	13.01 ± 2.75	12.48 ± 3.58	0.968
RAA indexed, cm^2/m^2	11.60 ± 2.91	11.39 ± 2.65	13.04 ± 4.63	11.97 ± 3.77	0.594
CMR variables					
MWT, mm	17.40 ± 2.96	17.64 ± 2.98	18.10 ± 4.07	19.89 ± 3.37	0.202
MWT indexed, mm/m^2	9.49 ± 1.88	9.66 ± 1.66	9.61 ± 2.29	10.25 ± 1.82	0.749
LV mass indexed, g/m^2	114.19 ± 20.1	119.45 ± 25.28	108.70 ± 27.02	139.67 ± 69.31	0.119
SV indexed, mL/m^2	36.74 ± 8.29	34.57 ± 9.94	34.00 ± 8.68	36.11 ± 8.70	0.724
EF, %	55.58 ± 10.40	56.75 ± 12.55	59.10 ± 9.75	53.89 ± 14.27	0.773
MAPSE, mm	6.53 ± 2.10	5.56 ± 1.97[b]	8.43 ± 1.81	8.71 ± 8.00	<0.001
TAPSE, mm	11.50 ± 5.10	11.00 ± 4.42	9.90 ± 4.56	13.44 ± 5.77	0.411
LAA indexed, cm^2/m^2	16.53 ± 2.78	16.84 ± 3.08	17.34 ± 2.65	15.68 ± 3.48	0.720
RAA indexed, cm^2/m^2	13.43 ± 2.53	14.09 ± 3.06	17.28 ± 5.16	13.42 ± 3.69	0.058
Native myocardial T1	1,182.32 ± 59.35	1,176 ± 55.56	1,134 ± 22.28	1,184 ± 51.18	0.095
Myocardial T2	52.19 ± 3.02	53.60 ± 3.72	49.50 ± 4.60	51.89 ± 4.54	0.066
LV LGE					0.719
None	0 (0.0)	0 (0.0)	0 (0.0)	0 (0.0)	
Subendocardial	7 (43.8)	10 (20.8)	2 (20.0)	3 (33.3)	
Transmural	24 (77.4)	38 (79.2)	8 (80.0)	6 (66.6)	
RV LGE	24 (77.4)	32 (66.7)	6 (60.0)	5 (55.6)	0.523
ECV	0.55 ± 0.07	0.55 ± 0.08	0.53 ± 0.09	0.55 ± 0.12	0.896

Values are mean ± SD, n (%), or median (IQR). *P* values for pairwise comparison: [a]$P < 0.05$ for grade 0 vs grade 1. [b]$P < 0.05$ for grade 1 vs grade 2.
Abbreviations as in Table 1.

early amyloid infiltration on CMR had normal cardiac structure and function but abnormal tissue characterization, with a higher native T1 and T2 than those with no CA, an elevated ECV, and subendocardial LGE. AL patients with grade 0 cardiac uptake and characteristic CMR features of CA had abnormal cardiac structure, with increased LV wall thickness and mass, impaired cardiac function, and further abnormalities in tissue characterization, with an even higher native T1 and T2, higher ECV, and higher prevalence of transmural LGE (Table 1).

TABLE 3 Baseline Characteristics and Echocardiographic and CMR Parameters for Patients With ATTR and Grade 1 Cardiac Uptake by ^{99m}Tc-DPD Scintigraphy, Separated by CMR Characteristics

	No Cardiac Amyloidosis (n = 25)	Early Cardiac Infiltration (n = 14)	Characteristic Cardiac Amyloidosis (n = 5)	*P* Value
Baseline characteristics				
Age, y	76.52 ± 11.88	76.04 ± 12.49	64.36 ± 8.54	0.113
Male	19 (76.0)	11 (78.6)	4 (80.0)	0.972
NYHA functional class				0.043
I	16 (64.0)[a]	6 (42.9)	0 (0.0)	
II	8 (32.0)[a]	6 (42.9)	5 (100.0)	
III	1 (4.0)	2 (14.3)	(0.0)	
IV	0 (0.0)	0 (0.0)	(0.0)	
NT-proBNP, pg/L	221 (124-863)	343 (83-1,512)	947 (440-5,488)	0.112
Troponin, ng/L	17 (12-25)	15 (9-31)	32 (23-69)	0.098
eGFR, mL/min/1.73 m^2	72 (65-87)	67 (55-86)	82 (73-90)	0.359
Echocardiographic variables				
IVSd, mm	11.52 ± 1.78[a]	12.21 ± 2.19[b]	16.00 ± 3.46	0.016
IVSd indexed, mm/m^2	6.09 ± 0.98[a]	6.40 ± 1.18[b]	8.76 ± 2.46	<0.001
PWTd, mm	11.08 ± 1.68[a]	11.57 ± 1.87[b]	15.50 ± 2.38	<0.001
PWTd indexed, mm/m^2	5.85 ± 0.10[a]	6.04 ± 1.28[b]	8.47 ± 1.84	<0.001
LS, %	−18.29 ± 3.38[a]	−17.88 ± 3.36[b]	−10.50 ± 3.15	0.010
E/A	0.83± 0.24	0.90 ± 0.28	1.10 ± 0.36	0.190
E/e′ average	9.08 ± 3.24	11.91 ± 10.10	14.73 ± 5.95	0.192
LAA indexed, cm^2/m^2	10.25 ± 3.13	11.15 ± 3.55	12.93 ± 3.69	0.303
RAA indexed, cm^2/m^2	8.28 ± 1.98	9.74 ± 3.21[b]	11.05 ± 2.61	0.119
CMR variables				
MWT, mm	11.50 ± 2.21[a]	13.92 ± 2.78[b]	17.25 ± 3.95	<0.001
MWT indexed, mm/m^2	5.74 ± 1.68[a]	6.68 ± 2.48[b]	9.45 ± 2.78	0.009
LV mass indexed, g/m^2	71.48 ± 18.80[a]	75.12 ± 15.18[b]	123.87 ± 68.23	0.001
SV indexed, mL/m^2	45.86 ± 9.51	46.89 ± 13.89	40.86 ± 5.66	0.298
EF, %	66.92 ± 10.35[a]	68.43 ± 7.70[b]	53.41 ± 11.16	0.562
MAPSE, mm	11.13 ± 2.34[a]	10.42 ± 2.88	7.40 ± 1.82	0.015
TAPSE, mm	21.91 ± 3.92	18.92 ± 5.71	16.40 ± 7.30	0.051
LAA indexed, cm^2/m^2	13.54 ± 2.66	13.46 ± 3.91	14.58 ± 1.90	0.828
RAA indexed, cm^2/m^2	11.89 ± 4.05	12.13 ± 4.37	12.92 ± 4.04	0.119
Native myocardial T1	999 ± 38[a]	1,048 ± 35[b]	1,091 ± 36	<0.001
Myocardial T2	48.53 ± 2.03	49.69 ± 1.60	47.50 ± 0.71	0.132
LV LGE				
None	25 (100.0)[a,c]	6 (42.9)	0 (0.0)	<0.001
Subendocardial	0 (0.0)[c]	8 (57.1)[b]	1 (20.0)	
Transmural	0 (0.0)[a]	0 (0.0)[b]	4 (80.0)	
RV LGE	0 (0.0)[c]	1 (7.1)[b]	3 (60.0)	<0.001
ECV	0.29 ± 0.02[a,c]	0.34 ± 0.01[b]	0.54 ± 0.09	<0.001

Values are mean ± SD, n (%), or median (IQR). *P* values for pairwise comparison: [a]$P < 0.05$ for no CA vs characteristic CA. [b]$P < 0.05$ for early CA vs characteristic CA. [c]$P < 0.05$ for no CA vs early CA.

ATTR = transthyretin amyloidosis; other abbreviations as in Table 1.

All 67 AL patients with ^{99m}Tc-DPD cardiac uptake (grade 1: n = 48; grade 2: n = 10; grade 3: n = 9) had characteristic CMR features of CA. They all had abnormal cardiac structure, impaired biventricular function, and grossly abnormal tissue characterization. Their cardiac biomarkers as well as echocardiography- and CMR-derived measures of cardiac structure, function, and tissue characterization were similar across the spectrum of cardiac uptake grades. Furthermore, there were no significant differences in cardiac structure, function, or tissue characterization between AL patients with grade 0 cardiac uptake and characteristic CMR features of CA and AL patients with grade 1, 2, or 3 (**Table 2,** Supplemental Figure 1).

TRANSTHYRETIN AMYLOIDOSIS. All ATTR patients with grade 0 cardiac uptake (n = 21) had no features of CA on CMR and had normal cardiac structure, function, and tissue characterization.

A total of 44 ATTR patients had grade 1 cardiac uptake, of whom 25 (56.8%; 95% CI: 41.0%-71.7%) had

FIGURE 2 **CMR Imaging in Grade 1 ^{99m}Tc-DPD Cardiac Uptake**

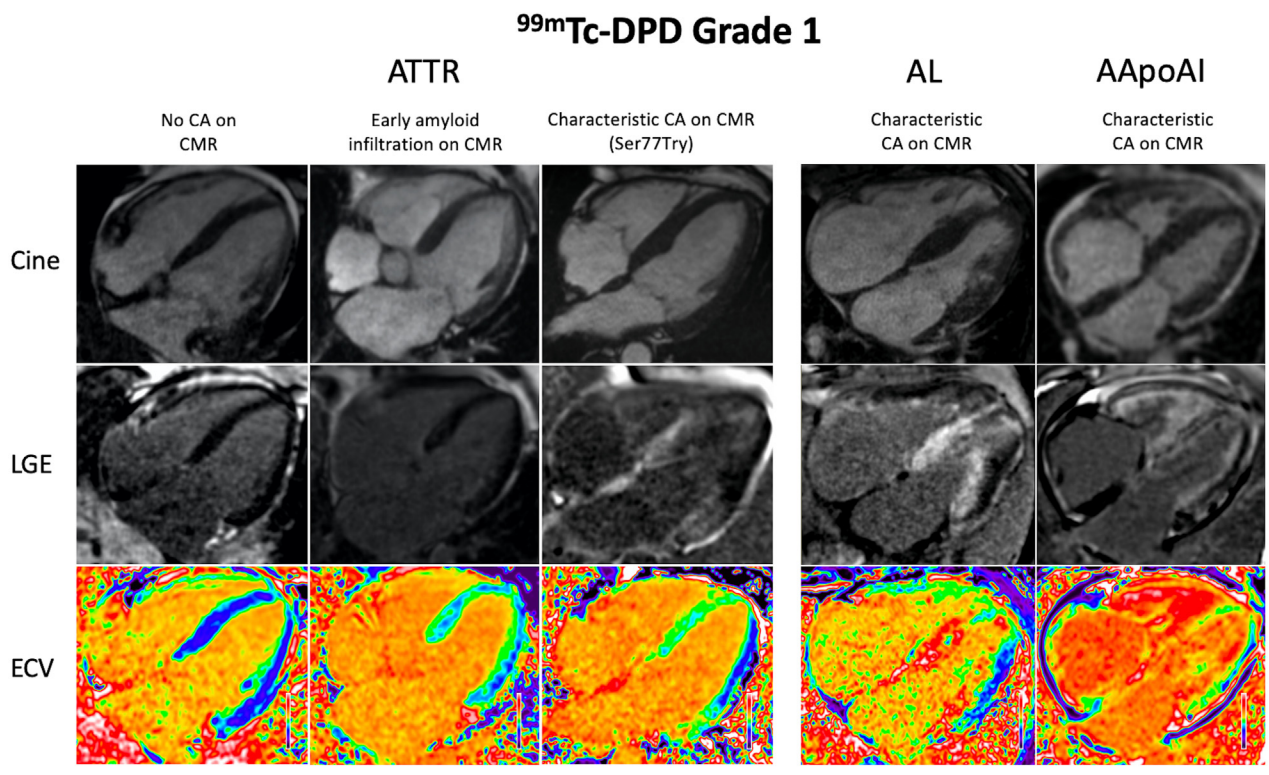

Images demonstrate the varying cardiac phenotype in patients with grade 1 ^{99m}Tc-DPD cardiac uptake. ^{99m}Tc-DPD = ^{99m}technetium-labeled 3,3-diphosphono-1,2-propanodicarboxylic acid; CA = cardiac amyloidosis; ECV = extracellular volume, LGE = late gadolinium enhancement; other abbreviations as in Figure 1.

no features of CA on CMR, 14 (31.8%; 95% CI: 18.6%-47.6%) had early cardiac amyloid infiltration, and 5 (11.4%; 95% CI: 3.8%-24.6%) had characteristic features of CA (all of whom had the S77Y *TTR* gene sequence variant). ATTR patients with grade 1 cardiac uptake and no CMR features of CA had normal cardiac structure, function, and tissue characterization. ATTR patients with grade 1 cardiac uptake and early amyloid infiltration had normal cardiac structure and function and early changes in tissue characterization with normal gadolinium kinetics, a mildly elevated ECV, and subtle subendocardial LV LGE in 57.1% (n = 8). All 5 ATTR patients with characteristic CA on CMR had Ser77Tyr hATTR and had abnormal cardiac structure with increased LV wall thickness and LV mass, impaired systolic function, and further increases in ECV and LGE (Table 3). When compared to all other ATTR patients with grade 1 cardiac uptake (n = 38), those with Ser77Tyr hATTR (n = 6) had a higher troponin-T (32 ng/L [23-69 ng/L] vs 17 ng/L [12-27 ng/L]; $P = 0.030$), increased wall thickness (maximal wall thickness [MWT]: 17.25 ± 3.95 mm vs 12.41 ± 2.67 mm; $P = 0.008$; MWT indexed: 9.44 ± 2.78 mm/m^2 vs 6.19 ± 1.06 mm/m^2; $P = 0.004$) and LV mass (114.34 ± 65.34 g/m^2 vs 72.94 ± 17.68 g/m^2; $P = 0.018$), and worse mitral annular plane systolic excursion (8.00 ± 2.19 mm vs 10.88 ± 2.56 mm; $P = 0.013$), longitudinal strain (LS) (−11.90 ± 4.15 vs −18.16 ± 3.38; $P = 0.002$), and LV ejection fraction (LVEF) (54.35% ± 10.24% vs 66.78% ± 9.42%; $P = 0.003$). Tissue characterization revealed that those with Ser77Tyr had more advanced cardiac amyloidosis, with an increased incidence of transmural LV LGE (4 [66.7%] vs 0 [0.0%]; $P < 0.001$) and right ventricle (RV) LGE (4 [66.7%] vs 0 [0.0%]; $P < 0.001$) and increased native T1 (1,081 ± 38 ms vs 1,016 ± 44 ms; $P = 0.003$) and ECV (0.51 ± 0.12 vs 0.31 ± 0.05; $P < 0.001$) (Figure 2).

When comparing ATTR patients with grade 0 cardiac uptake to ATTR patients with grade 1, there were no significant differences in cardiac structure or function, but those with grade 1 had

TABLE 4 Baseline Characteristics and Echocardiographic and CMR Parameters for Patients With Cardiac ATTR Across All ^{99m}Tc-DPD Scintigraphy Grades

	Grade 0 (n = 21)	Grade 1 (n = 44)	Grade 2 (n = 50)	Grade 3 (n = 50)	*P* Value
Baseline characteristics					
Age, y	61.75 ± 19.36[a,b]	73.98 ± 12.15	76.01 ± 7.61	73.62 ± 11.05	0.020
Male	10 (47.6)[b,c]	34 (77.3)	44 (88.0)	39 (78.0)	0.003
NYHA functional class					<0.001
I	18 (85.7)[a,b,c]	22 (50.0)[d,e]	4 (8.0)	2 (4.0)	
II	3 (14.3)[b,c]	19 (43.2)[d,e]	45 (90.0)	37 (74.0)	
III	0 (0.0)	3 (6.8)[e]	1 (2.0)[f]	10 (20.0)	
IV	0 (0.0)	0 (0.0)	0 (0.0)	0 (0.0)	
NT-proBNP, pg/L	68 (34-305)[b,c]	247 (123-979)[d,e]	2,114 (1,227-4,419)	2,523 (1,421-4,977)	<0.001
Troponin, ng/L	3 (2-14)[a,b,c]	18 (12-31)[d,e]	58 (34-78)	64 (46-87)	<0.001
eGFR, mL/min/1.73 m^2	82 (69-90)[c]	72 (65-87)	72 (52-87)	62 (46-81)	0.007
Echocardiographic variables					
IVSd, mm	10.14 ± 1.24[b,c]	12.16 ± 2.41[d,e]	16.22 ± 2.67	17.68 ± 2.82	<0.001
IVSd indexed, mm/m^2	5.39 ± 0.95[b,c]	6.43 ± 1.42[d,e]	8.58 ± 1.41[f]	9.87 ± 1.86	<0.001
PWTd, mm	9.48 ± 1.33[a,b,c]	11.65 ± 2.17[d,e]	16.10 ± 2.54[f]	17.42 ± 2.49	<0.001
PWTd indexed, mm/m^2	5.04 ± 1.04[a,b,c]	6.17 ± 1.36[d,e]	8.52 ± 1.41[f]	9.76 ± 1.80	<0.001
LS, %	−18.38 ± 3.63[b,c]	−17.31 ± 4.05[d,e]	−11.20 ± 3.72[f]	−8.33 ± 2.90	<0.001
E/A	1.19 ± 0.37[b,c]	0.89 ± 0.27[d,e]	2.23 ± 1.13	2.20 ± 1.03	<0.001
E/e′ average	8.94 ± 4.54[b,c]	10.56 ± 6.67[d,e]	16.78 ± 1.14	18.86 ± 6.76	<0.001
LAA indexed, cm^2/m^2	9.54 ± 3.93[b,c]	10.81 ± 3.34[d,e]	13.96 ± 2.53	14.03 ± 3.20	<0.001
RAA indexed, cm^2/m^2	8.90 ± 2.36[b,c]	9.02 ± 2.62[d,e]	12.52 ± 2.52	13.10 ± 3.60	<0.001
CMR variables					
MWT, mm	10.18 ± 2.46[a,b,c]	12.94 ± 3.17[d,e]	17.28 ± 3.33[f]	20.50 ± 3.66	<0.001
MWT indexed, mm/m^2	4.99 ± 1.53[b,c]	6.45 ± 2.33[d,e]	9.13 ± 1.72[f]	11.43 ± 2.27	<0.001
LV mass indexed, g/m^2	65.22 ± 14.63[b,c]	78.59 ± 31.17[d,e]	125.52 ± 34.51	155.37 ± 39.94	<0.001
SV indexed, mL/m^2	47.00 ± 6.88[b,c]	45.61 ± 10.72[d,e]	36.48 ± 8.93	35.63 ± 8.65	<0.001
EF, %	68.90 ± 6.37[b,c]	65.86 ± 10.49[d,e]	56.86 ± 14.70[f]	49.38 ± 12.56	<0.001
MAPSE, mm	12.65 ± 2.62[b,c]	10.77 ± 2.82[d,e]	6.96 ± 2.24	6.50 ± 2.12	<0.001
TAPSE, mm	21.85 ± 4.76[b,c]	20.70 ± 5.27[d,e]	12.18 ± 4.04	10.84 ± 3.75	<0.001
LAA indexed, cm^2/m^2	13.55 ± 4.52[b,c]	13.63 ± 3.00[d,e]	16.83 ± 3.27	16.43 ± 2.85	<0.001
RAA indexed, cm^2/m^2	12.00 ± 2.64[b,c]	12.09 ± 4.06[d,e]	15.14 ± 3.54	16.00 ± 3.21	<0.001
Native myocardial T1	995 ± 51.18[b,c]	1023 ± 48.10[d,e]	1131 ± 44.26	1145 ± 54.67	<0.001
Myocardial T2	49.01 ± 2.20[c]	48.91 ± 1.91[e]	48.90 ± 2.86[f]	52.53 ± 3.94	<0.001
LV LGE					<0.001
None	21 (100.0)[a,b,c]	31 (70.5) [d,e]	0 (0.0)	0 (0.0)	
Subendocardial	0 (0.0)[b]	9 (20.5)[e]	23 (46.0)[f]	3 (6.0)	
Transmural	0 (0.0)[b,c]	4 (9.1)[d,e]	27 (54.0)[f]	47 (94.0)	
RV LGE	0 (0.0)[b,c]	4 (9.1)[d,e]	46 (92.0)	49 (98.0)	<0.001
ECV	0.28 ± 0.02[b,c]	0.34 ± 0.09[d,e]	0.53 ± 0.08[f]	0.68 ± 0.08	<0.001

Values are mean ± SD, n (%), or median (IQR). *P* values for pairwise comparison: [a]$P < 0.05$ for grade 0 vs grade 1. [b]$P < 0.05$ for grade 0 vs grade 2. [c]$P < 0.05$ for grade 0 vs grade 3. [d]$P < 0.05$ for grade 1 vs grade 2. [e]$P < 0.05$ for grade 1 vs 3. [f]$P < 0.05$ for grade 2 vs grade 3.

Abbreviations as in Tables 1 and 3.

early changes in tissue characterization, with an increase ECV and subtle LGE in a proportion of patients.

All ATTR patients with grade 2 cardiac uptake (n = 50) and grade 3 cardiac uptake (n = 50) had characteristic features of CA, with increased LV wall thickness and LV mass, impaired cardiac function, diffuse LGE, and an elevated ECV. When comparing ATTR patients with grade 2 cardiac uptake to ATTR patients with grade 3, those with grade 3 had an increased MWT; reduced LVEF; worse LS; and, on tissue characterization, a higher T2, higher ECV, and greater degree of LV LGE transmurality.

As ATTR patients progressed from grade 1 to grade 2 cardiac uptake, they developed abnormal cardiac structure with increased LV wall thickness and LV mass; abnormal cardiac function with impaired biventricular systolic function and LV diastolic dysfunction; and further abnormalities in tissue characterization, with increased native T1, LGE, and

FIGURE 3 **Multimodality Imaging in AApoAI**

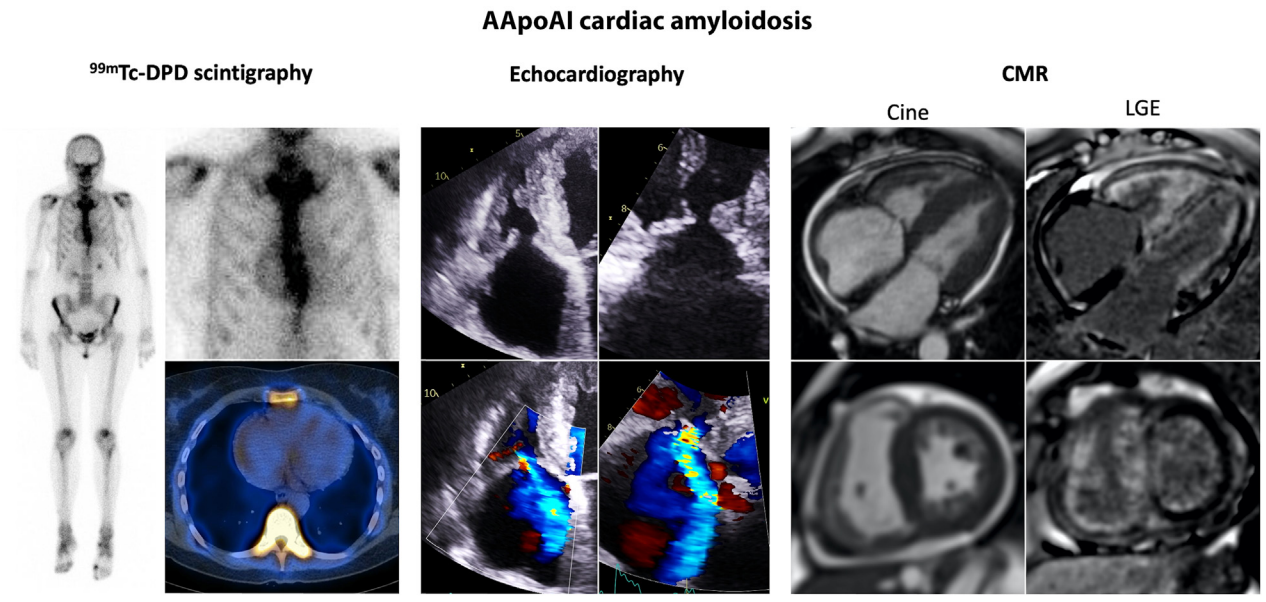

Images demonstrate the characteristic features identified in patients with AApoAI. Abbreviations as in Figures 1 and 2.

ECV. As ATTR patients progressed to grade 3, their cardiac structure became more abnormal, with further increases in LV wall thickness and LV mass; cardiac function deteriorated further, with worsening of LVEF and LS; and tissue characterization became more abnormal, with a further increase in LGE, ECV, and myocardial T2 (Table 4).

APOLIPOPROTEIN AI AMYLOIDOSIS. In AApoAI patients, 3 (42.9%; 95% CI: 9.9%-81.6%) had grade 0 cardiac uptake, and 4 (57.1%; 95% CI: 18.4%-90.1%) had grade 1. Only 1 patient (who was grade 0) had no CMR features of CA and had normal cardiac structure, function, and tissue characterization. The remaining 6 patients, all had either early features of amyloid infiltration (n = 4) with normal LV structure and function but abnormal tissue characterization or had characteristic CMR features of CA (n = 2) with abnormal LV structure, function, and tissue characterization (LV LGE: 6 [100%]; transmural LGE: 2 [33.3%]; ECV: 0.44 ± 0.07).

Patients with AApoAI had unique features of disproportionate right-sided involvement: 1) RV free wall thickening (8.00 ± 2.00 mm), RV LGE (n = 6; 100%), and disproportionate RV uptake on ^{99m}Tc-DPD SPECT (n = 3; 75%); 2) disproportionate right atrium (RA) wall thickening and RA uptake on ^{99m}Tc-DPD SPECT (n = 3; 75%); and 3) severe thickening of the tricuspid valve and subvalvular apparatus (n = 5), 80% (n = 4) of whom had tethering of the septal tricuspid valve leaflet and eccentric regurgitation (mild: n = 3; severe: n = 1) (Figure 3).

APOLIPOPROTEIN AIV AMYLOIDOSIS. All 7 patients with AApoAIV had grade 0 cardiac uptake and characteristic CMR features of CA. All 7 AApoAIV patients had abnormal cardiac structure with increased LV wall thickness (MWT: 19.67 ± 4.27 mm; MWT indexed: 9.01 ± 4.58 mm/m^2), LV mass (141.28 ± 30.83 g/m^2), and biatrial area (left atrium: 17.75 ± 2.84 cm^2/m^2; RA: 14.03 ± 2.98 cm^2/m^2); abnormal biventricular systolic function (mitral annular plane systolic excursion: 5.67 ± 2.16 mm; tricuspid annular plane systolic excursion: 13.00 ± 4.90; LS: −10.67% ± 1.60%); and abnormal tissue characterization, with elevated native T1 (1,140 ± 55 ms), elevated ECV (0.56 ± 0.09), and biventricular LGE in all 7 (100.0%) patients (transmural LV LGE: 4; 57.1%). These findings were accompanied by elevated serum cardiac biomarkers (N-terminal pro-B-type natriuretic peptide: 4,416 pg/L [IQR: 2,926-4,939 pg/L]; troponin-T: 48 ng/L [IQR: 36.0-123.0 ng/L]).

COMPARISON BETWEEN DIFFERENT TYPES OF AMYLOIDOSIS. ATTR with grade 0 cardiac uptake had no CA on CMR, whereas AL and AApoAI spanned the spectrum from no CA to characteristic features of CA, and all AApoAIV patients had characteristic features of CA.

AL with grade 1 cardiac uptake had characteristic CMR features of CA, whereas only ATTR with Ser77-Tyr had characteristic CMR features of CA. The

JACC: CARDIOVASCULAR IMAGING, VOL. 16, NO. 4, 2023
APRIL 2023:464–477

FIGURE 4 ECV and ^{99m}Tc-DPD Grade

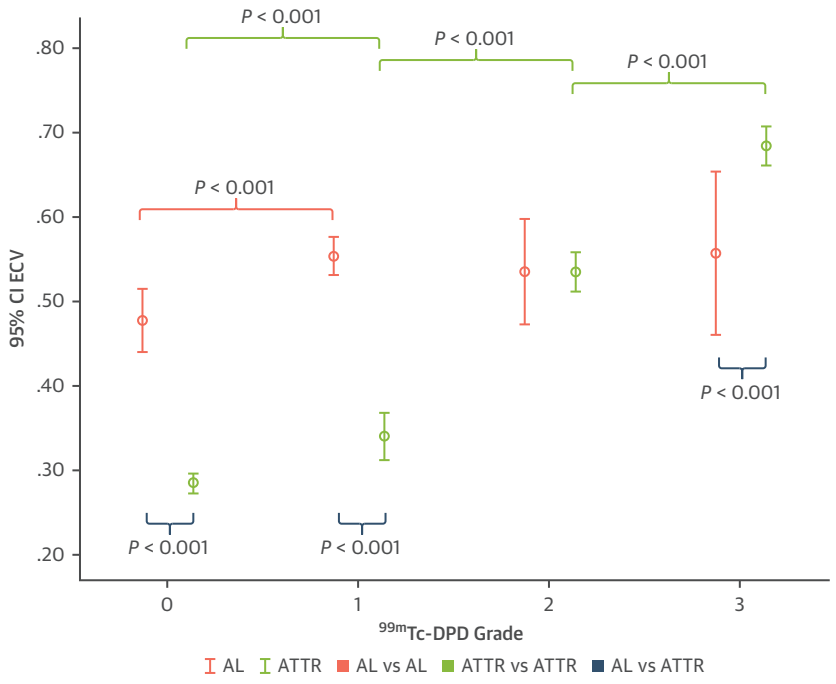

Error bars demonstrating the differences in ECV across different grades of ^{99m}Tc-DPD cardiac uptake in AL and ATTR. Abbreviations as in Figures 1 and 2.

remaining ATTR patients with grade 1 had either no CA or early amyloid infiltration, whereas those with AApoAI had predominantly RV involvement.

In grade 1 cardiac uptake, following the exclusion of AApoAI and AApoAIV, the underlying type can be determined by CMR and genetic screening. Within our study population, following exclusion of Ser77Tyr and AApoAI, CMR showing no features of CA or early amyloid infiltration has a sensitivity and specificity of 100% for ATTR, whereas CMR showing characteristic features of CA has a sensitivity and specificity of 100% for AL.

ECV is an excellent discriminator between ATTR and AL with grade 1 cardiac uptake. Once Ser77Tyr and AApoAI have been excluded, an ECV of <0.40 has a sensitivity and specificity of 100% for ATTR, and an ECV of >0.40 has a sensitivity and specificity of 100% for AL.

At grade 2 and 3 cardiac uptake, there were no significant differences in structural or functional cardiac imaging parameters between AL and ATTR when matched for cardiac uptake grade. However, ATTR patients with grade 3 uptake had a higher ECV than AL patients (0.68 ± 0.08 vs 0.55 ± 0.12; $P < 0.001$).

ATTR had a stronger correlation between ^{99m}Tc-DPD cardiac uptake and measures of cardiac structure, function, and tissue characterization than AL. This was most pronounced in ECV quantification (ATTR: $R = 0.88$; 95% CI: 0.84-0.91; $P < 0.001$; AL: $R = 0.26$; 95% CI: 0.08-0.42; $P = 0.006$) (Figure 4).

DISCUSSION

To our knowledge, this is the first study to produce a deep multi-imaging characterization of cardiac phenotype in different amyloidosis types across a range of ^{99m}Tc-DPD cardiac uptake grades. Our study demonstrated the following: 1) AL grade 0 patients span the spectrum of CMR findings, from no CA to characteristic features of CA, whereas AL grade 1 to 3 patients always produce characteristic CMR features; 2) in ATTR, the CA burden strongly correlates with cardiac uptake grade, except in Ser77Tyr hATTR; 3) AApoAI and AApoAIV should be considered in grade 0 patients and AApoAI in grade 1, especially when features such as disproportionate right-sided involvement (RV wall thickening and LGE, right atrium wall thickening and tricuspid valve

CENTRAL ILLUSTRATION **Diagnostic Pathway for Patients With Characteristic Features of CA on CMR**

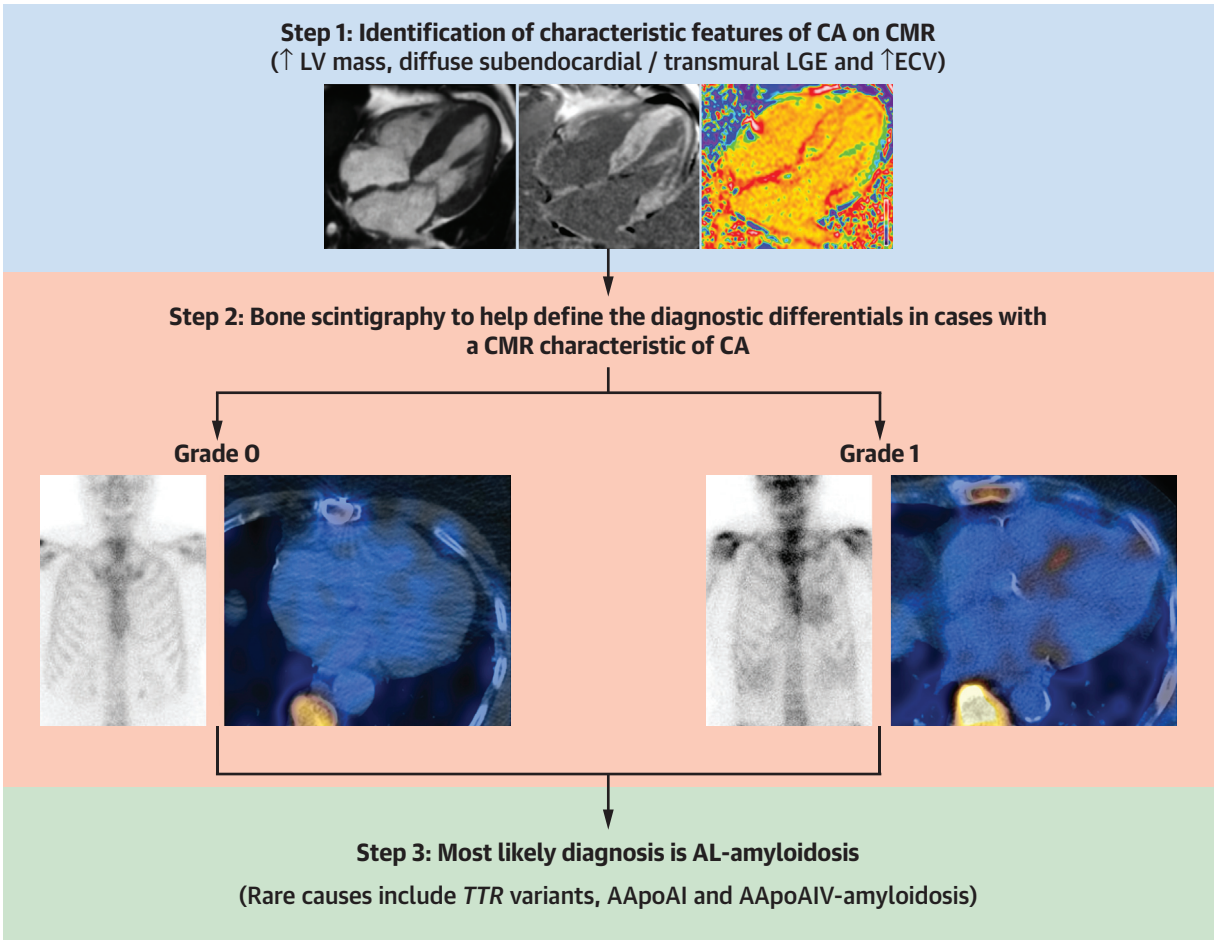

Ioannou A, et al. J Am Coll Cardiol Img. 2023;16(4):464–477.

The identification of distinctive characteristics allowed the development of a pathway to help differentiate different types of amyloidosis following comprehensive assessment with ^{99m}technetium-labeled 3,3-diphosphono-1,2-propanodicarboxylic acid scintigraphy and CMR. This pathway should only be used in patients with a CMR characteristic of CA. Although there were no cases in our study cohort, there have been sparse reports of mild myocardial tracer uptake in apolipoprotein AIV amyloidosis (AApoAIV). AL = immunoglobulin light-chain amyloidosis; AApoAI = apolipoprotein AI amyloidosis; CA = cardiac amyloidosis; CMR = cardiac magnetic resonance; ECV = extracellular volume; LGE = late gadolinium enhancement; LV = left ventricle.

thickening/dysfunction) are identified; and 4) A combination of ^{99m}Tc-DPD scintigraphy and CMR in patients with grade 0 or 1 cardiac uptake on ^{99m}Tc-DPD scintigraphy may refine diagnostic pathways in CA, but this requires validation in larger studies.

AL patients with grade 0 cardiac uptake can have no CA, early features of amyloid infiltration, or characteristic CA; hence, ^{99m}Tc-DPD scintigraphy has a low sensitivity for detecting AL-CA. There is no difference in the cardiac phenotype between AL patients with characteristic CA on CMR who are grade 0 and those who are grade 1, 2, or 3; however, all patients with ^{99m}Tc-DPD uptake had characteristic CMR features of CA. Therefore, in AL, ^{99m}Tc-DPD uptake is not representative of the degree of cardiac amyloid infiltration, and importantly, grade 0 cardiac uptake does not exclude CA. Consequently, in cases where there is a high pretest probability of systemic AL, bone scintigraphy alone should not be used to determine the presence or severity of CA.

The ATTR-amyloid burden strongly correlates with ^{99m}Tc-DPD cardiac uptake grade (Figure 4), except for in Ser77Tyr. In ATTR patients with grade 0, there are no features of CA on CMR. In ATTR patients with

grade 1 (excluding Ser77Tyr), there are very early changes representative of amyloid deposits within the myocardium, whereas all echocardiography- and CMR-derived measures of cardiac structure and function remain normal. All ATTR patients with cardiac uptake grade 2 or 3 had characteristic features of CA, with abnormal cardiac structure, function, and tissue characterization. In the last few years, there has been a significant increase of patients with ATTR and grade 1 cardiac uptake. This has been associated with the need to define this phenotype and establish where this phenotype is on the spectrum of cardiac amyloid infiltration.

Our study has shown significant differences between patients with ATTR, with the cardiac uptake ranging from grade 1 to grade 3. Patients with ATTR and grade 1 cardiac uptake have evidence of very early amyloid deposits that can only be identified on tissue characterization, with no significant changes in structure and function, whereas those with grade 2 or 3 cardiac uptake have developed an established and extensive disease process associated with all the typical functional and structural changes typical of cardiac amyloidosis. The only exception to this was patients with ATTR associated with the variant Ser77Tyr, in whom there was good agreement between the characteristic CMR findings, cardiac biomarkers, and echocardiographic measures of CA burden despite a disproportionately low cardiac uptake on ^{99m}Tc-DPD.[18] The less-than-expected ^{99m}Tc-DPD uptake has also been reported in patients with the rare pathogenic Phe64Leu[19] and Y114C *TTR* variants[20] as well as some patients with Val30Met; all of these variants are associated with type-B amyloid fibrils, suggesting that the degree of uptake is variant dependent. This further emphasizes the importance of genetic testing in patients with suspected CA but low or absent ^{99m}Tc-DPD cardiac uptake.

We extensively characterized the cardiac phenotype in patients with AApoAI and AApoAIV and identified that both subtypes can present as ^{99m}Tc-DPD cardiac uptake grade 0 and that AApoAI can also present with grade 1 uptake. AApoAI CA produces distinctive features of disproportionate right-sided involvement comprising RV free wall thickening, RV ^{99m}Tc-DPD uptake, and LGE; RA wall thickening and ^{99m}Tc-DPD uptake; tricuspid valve thickening; and septal leaflet tethering, resulting in restricted mobility and eccentric regurgitation (**Figure 3**). If seen, these novel findings should prompt genetic screening for underlying AApoAI.

The diagnostic pathway for ^{99m}Tc-DPD cardiac uptake of grades 2 and 3 is well established,[5] but grade 0 and 1 patients still present a diagnostic challenge.[6] Our study has shown that all patients with AL and grade 1 ^{99m}Tc-DPD cardiac uptake have a severe burden of CA on CMR, whereas grade 1 ATTR patients (with the exception Ser77-Tyr) have minimal CA on CMR (**Figure 2**)—that is, only early changes in the tissue characterization, which include mild elevation in ECV or very subtle subendocardial LGE. Furthermore, the combination of grade 0 cardiac uptake on ^{99m}Tc-DPD and a characteristic CMR is consistent with cardiac AL, with the only exceptions being AApoAI and AApoAIV. Therefore, in the presence of characteristic features of CA on CMR or an ECV of >0.40 and ^{99m}Tc-DPD cardiac uptake of grade 0 or 1, the most likely diagnosis is cardiac AL (**Central Illustration**). It is important to emphasize that in patients with a high pretest probability of AL, the use of standalone bone scintigraphy to determine cardiac amyloid infiltration is not recommended, whereas the combination of CMR and bone scintigraphy can help to define the diagnostic differentials and the clinical phenotype for each individual patient. However, this requires validation in larger studies.

STUDY LIMITATIONS. The main limitation of our study is that it is a single-center study with a small sample size, but this reflects the rare nature of these diseases and probably represents an unavoidable limitation. Because this was not a population study, we are unable to comment on the overall prevalence of ^{99m}Tc-DPD in different types of amyloidosis. The main exclusion criterion was gadolinium contrast not being administered during CMR, often because of chronic kidney disease. Omission of these patients may have inadvertently excluded those with more severe systemic disease. This would have particularly affected those with AL[1,6] and AApoAIV,[10] in whom renal involvement is common. Therefore, our results can be extrapolated only to patients who receive gadolinium contrast. Finally, although the sensitivity and specificity of bone tracers are similar for diagnosing ATTR, our findings cannot necessarily be extrapolated to bone tracer agents other than ^{99m}Tc-DPD.

CONCLUSIONS

Deep characterization of the cardiac phenotype in different amyloidoses, across a range of ^{99m}Tc-DPD cardiac uptake grades, has identified clear differences among the amyloidosis types. The distinctive

characteristics in each cohort can help differentiate patients following comprehensive assessment with ^{99m}Tc-DPD scintigraphy and CMR, but this will require further validation.

FUNDING SUPPORT AND AUTHOR DISCLOSURES

Dr Fontana is supported by a British Heart Foundation Intermediate Clinical Research Fellowship (FS/18/21/33447). All other authors have reported that they have no relationships relevant to the contents of this paper to disclose.

ADDRESS FOR CORRESPONDENCE: Dr Marianna Fontana, National Amyloidosis Centre, University College London, Royal Free Hospital, Rowland Hill Street, London NW3 2PF, United Kingdom. E-mail: m.fontana@ucl.ac.uk.

PERSPECTIVES

COMPETENCY IN MEDICAL KNOWLEDGE: Deep characterization of the cardiac phenotype in different amyloidosis types, across a range of ^{99m}Tc-DPD cardiac uptake grades, has identified clear differences between each cohort, including the description of novel features characteristic of AApoAI CA.

TRANSLATIONAL OUTLOOK: The identification of distinctive characteristics could allow the development of a diagnostic pathway to help differentiate patients following comprehensive assessment with ^{99m}Tc-DPD scintigraphy and CMR. Validation in a multicenter prospective study could refine diagnostic pathways in CA and negate the need for a biopsy.

REFERENCES

1. Ioannou A, Patel R, Gillmore JD, et al. Imaging-guided treatment for cardiac amyloidosis. *Curr Cardiol Rep*. 2022;24(7):839–850. https://doi.org/10.1007/s11886-022-01703-7

2. Fontana M, Ćorović A, Scully P, et al. Myocardial amyloidosis: the exemplar interstitial disease. *J Am Coll Cardiol Img*. 2019;12:2345–2356.

3. Eriksson M, Schönland S, Yumlu Sal. Hereditary apolipoprotein AI-associated amyloidosis in surgical pathology specimens: identification of three novel mutations in the APOA1 gene. *J Mol Diagn*. 2009;11(3):257–262.

4. Bois MC, Dasari S, Mills JR, et al. Apolipoprotein A-IV-associated cardiac amyloidosis. *J Am Coll Cardiol*. 2017;69:2248–2249.

5. Gillmore JD, Maurer MS, Falk RH, et al. Non-biopsy diagnosis of cardiac transthyretin amyloidosis. *Circulation*. 2016;133:2404–2412.

6. Quarta CC, Zheng J, Hutt D, et al. 99mTc-DPD scintigraphy in immunoglobulin light chain (AL) cardiac amyloidosis. *Eur Heart J Cardiovasc Imaging*. 2021;22:1304–1311.

7. Rapezzi C, Quarta CC, Guidalotti PL, et al. Role of 99mTc-DPD scintigraphy in diagnosis and prognosis of hereditary transthyretin-related cardiac amyloidosis. *J Am Coll Cardiol Img*. 2011;4:659–670.

8. Quarta CC, Obici L, Guidalotti PL, et al. High 99mTc-DPD myocardial uptake in a patient with apolipoprotein AI-related amyloidotic cardiomyopathy. *Amyloid*. 2013;20:48–51.

9. Saleem M, Balla S, Amin MS, et al. Hereditary apolipoprotein A-I–associated cardiac amyloidosis: importance of endomyocardial biopsy when suspicion remains high. *J Am Coll Cardiol Case Rep*. 2021;3(7):1032–1037.

10. Martins E, Urbano J, Leite S, et al. Cardiac amyloidosis associated with apolipoprotein A-IV deposition diagnosed by mass spectrometry-based proteomic analysis. *Eur J Case Rep Intern Med*. 2019;6(12):001237.

11. Garcia-Pavia P, Rapezzi C, Adler Y, et al. Diagnosis and treatment of cardiac amyloidosis: a position statement of the ESC Working Group on Myocardial and Pericardial Diseases. *Eur Heart J*. 2021;42:1554–1568.

12. Dorbala S, Ando Y, Bokhari S, et al. ASNC/AHA/ASE/EANM/HFSA/ISA/SCMR/SNMMI expert consensus recommendations for multimodality imaging in cardiac amyloidosis: part 2 of 2—diagnostic criteria and appropriate utilization. *J Card Fail*. 2019;25:854–865.

13. Perugini E, Guidalotti PL, Salvi F, et al. Noninvasive etiologic diagnosis of cardiac amyloidosis using 99mTc-3,3-diphosphono-1,2-propanodicarboxylic acid scintigraphy. *J Am Coll Cardiol*. 2005;46:1076–1084.

14. Hawkins PN, Lavender JP, Pepys MB. Evaluation of systemic amyloidosis by scintigraphy with 123I-labeled serum amyloid P component. *N Engl J Med*. 1990;323:508–513.

15. Chacko L, Martone R, Bandera F, et al. Echocardiographic phenotype and prognosis in transthyretin cardiac amyloidosis. *Eur Heart J*. 2020;41:1439–1447a.

16. Kellman P, Hansen MS. T1-mapping in the heart: accuracy and precision. *J Cardiovasc Magn Reson*. 2014;16(1):2.

17. White SK, Sado DM, Fontana M, et al. T1 mapping for myocardial extracellular volume measurement by CMR: bolus only versus primed infusion technique. *J Am Coll Cardiol Img*. 2013;6:955–962.

18. Martinez-Naharro A, Treibel TA, Abdel-Gadir A, et al. Magnetic resonance in transthyretin cardiac amyloidosis. *J Am Coll Cardiol*. 2017;7:466–477.

19. Musumeci MB, Cappelli F, Russo D, et al. Low sensitivity of bone scintigraphy in detecting Phe64Leu mutation-related transthyretin cardiac amyloidosis. *J Am Coll Cardiol Img*. 2020;13:1314–1321.

20. Pilebro B, Suhr OB, Näslund U, et al. 99mTc-DPD uptake reflects amyloid fibril composition in hereditary transthyretin amyloidosis. *Ups J Med Sci*. 2016;121(1):17–24.

KEY WORDS bone scintigraphy, cardiac amyloidosis, cardiac magnetic resonance

APPENDIX For an expanded Methods section as well as a supplemental figure, please see the online version of this paper.